This chapter is part of a Ph.D. Thesis

Available on : http://edoc.bib.ucl.ac.be

Acid Neutralization and Sulphur retention in S-impacted Andosols

THOMAS DELFOSSE

MAY 2005

Université catholique de Louvain
Faculté d'ingénierie biologique, agronomique et environnementale
Département des sciences du milieu et de l'aménagement du territoire
Unité des sciences du sol

Croix du Sud, 2/10, 1348 Louvain-la-Neuve, Belgium
Tél. 32 (0) 10 47 36 33 – Fax 32 (0) 10 47 45 25
E-mail : delvaux@sols.ucl.ac.be - delfosse@sols.ucl.ac.be
http://www.sols.ucl.ac.be

This Chapter is also adapted from
Delfosse T., Delmelle P., Iserentant A. & Delvaux B. 2005. SO3 contribution to Acid neutralizing capacity of Andosols exposed to strong volcanogenic acid and SO2 deposition. European Journal of Soil Science, 56, 113-125.
Available on : http://www.blackwell-synergy.com/rd.asp?code=EJS&goto=journal

Part I

Acid Neutralising Mechanisms and Fates of SO_4^{2-}, F^- and Cl^-

Chapter 3

Acid Neutralising Capacity of Masaya Andosols*

Summary

Soil response to acid and sulphur inputs is influenced largely by the soil's physico-chemical properties. We studied the effects of such depositions in two types of Andosols exposed to volcanogenic emission (Masaya, Nicaragua), namely Eutric Andosols rich in allophanic constituents, and Vitric Andosols rich in volcanic glass. Small mineral reserves and large contents of secondary short-range ordered minerals indicate a more advanced weathering of the Eutric than the Vitric Andosols. Strong correlations between soil specific surface and oxalate-extractable Al, Si and Fe contents highlight the predominant contribution of short-range ordered minerals to surface area.

Prolonged acid inputs have led to a general pH decrease and reduced exchangeable base cation concentrations in both types of Andosols. Sulphur deposition increased the soil's S content to 5470 mg S kg^{-1}. However, the acid neutralising capacity of the soil solid phase (ANC_s) was not significantly affected by the acid and S inputs. Non-exchangeable (mineral reserve) and exchangeable cations and total contents of sulphur and phosphorus dictate most of the ANC_s variation. In the Vitric Andosols, mineral reserves contributed up to 97% to these four additive pools, whereas the exchangeable cations accounted for 1-4%. In the Eu-

*Adapted from (i) Delfosse T., Delmelle P., Iserentant A. & Delvaux B. 2005. SO_3 contribution to Acid neutralizing capacity of Andosols exposed to strong volcanogenic acid and SO_2 deposition. *European Journal of Soil Science*, **56**, 113-125, and (ii) Delmelle P., Delfosse T. & Delvaux B. 2003. Sulfate, chloride and fluoride retention in Andosols exposed to volcanic acid emissions. *Environmental Pollution*, **126**, 445-457.

tric Andosols, the contribution of mineral reserves was less (71-92%), but the exchangeable cation content was greater (1-20%), whereas the contribution of sulphur and phosphorus was significant at 1-15% and 2-7%, respectively. The main process involved in H^+ consumption is mineral weathering in Vitric Andosols and ion exchange in Eutric Andosols.

3.1 Introduction

Sulphur releases from metal smelters and coal-power plants contributes to regional atmospheric acid deposition (Arndt *et al.*, 1997). It is well established that anthropogenic acid loading has increased sulphate and proton fluxes through soils in affected areas, eventually enhancing soil acidification. Soil acidification remains an environmental issue, both in industrial and in less-developed countries (Alewell *et al.*, 2000), because it alters soil and water properties, thus potentially modifying current processes in whole ecosystems (Ulrich, 1991).

The capacity of a soil to neutralise acid inputs depends mainly on reactions involving mineral weathering and cation exchange, in which protons are consumed, and to a lesser extent on the selective retention of anions which reduces leaching of cations through the soil profile (Rajan, 1978; Bloom, 2000). The acid neutralising capacity of the soil solid phase (ANC_s) correlates positively with total Ca, Mg, K, Na, Al, Fe and Mn contents, but negatively with total P, S and Cl contents (van Breemen *et al.*, 1983) and has been successfully used to evaluate the degree of soil acidification (Brahy *et al.*, 2000).

There are many studies on soil acidification in forest soils from North America and Europe. In contrast, the response of Andosols, with their distinct chemical and mineral properties, to increased atmospheric acid deposition has been investigated only recently in areas of Japan and southeast Asia (e.g. Shindo *et al.*, 1995). Most Andosols are typically characterised by large mineral reserves, which give rise to a large ANC_s, and are rich in allophanic and other secondary short-range ordered minerals (Shoji *et al.*, 1993). These minerals exhibit a large cation exchange capacity (CEC), as well as a specific anionic retention, with the latter being pH-dependent (Shoji *et al.*, 1993). Combined with a high CEC, the large ANC_s found in Andosols should make them relatively insensitive to acidification. In addition, the large capacity of Andosols to retain various anions, including sulphate, may also delay net acidification (Rajan, 1978).

Andosols exhibiting various degrees of weathering occur in regions covered by volcanic tephra (Shoji *et al.*, 1993). Interestingly, many vol-

canoes are still active in these areas, and they sometimes release large amounts of sulphurous and halogenated acid compounds (mainly SO_2, H_2S, HCl and HF) into the atmosphere. In fact, there is increasing evidence that these volcanic emissions enhance acid deposition significantly, both locally and regionally (Parnell, 1986; Arndt *et al.*, 1997; Delmelle *et al.*, 2001). Thus, Andosols near active volcanoes can receive large inputs of sulphur and acids for many years. Such environments provide opportunity to study the short and long-term response of Andosols to intense acid loading.

We have studied the contrasting effects of sulphur and proton inputs on the acidification of two types of Andosols, both developed in similar basaltic ash, but differing in weathering stage. Both soils are downwind of a degassing volcano in Nicaragua and have undergone strong acid deposition for at least 150 years (Stoiber *et al.*, 1986; Delmelle *et al.*, 2002). To identify the major sinks of protons and sulphur in these Andosols, we assessed the weathering stage of the soils from the total contents of alkali and alkaline-earth cations, and we calculated the ANC_S by considering the phosphorus and sulphur contents. We report our results below.

3.2 Environmental setting

The study area is southwest of the Masaya caldera, a basaltic complex about 20 km from Managua, the capital of Nicaragua. The current activity of the Masaya volcano makes it one of the world's largest sources of SO_2. It also contributes significant amounts of halogens (as HCl and HF) to the troposphere (Delmelle *et al.*, 2001).

Transport of the Masaya emissions downwind gives large ambient concentrations of SO_2, leading to enhanced SO_2 deposition within a 1250-km^2 area (Delmelle *et al.*, 2001). The dispersion of the plume is strongly influenced by local topography (Delmelle *et al.*, 2002). The degassing crater (560 m above sea level) inside the caldera is actually lower than the western caldera ridge (at 580 m). Approximately 15 km west, the Llano Pacaya ridge (700-920 m) is another prominent topographic feature (Figures 2.9 and 3.2). Reported values of SO_2 dry-deposition range between 200 and 700 mg SO_2 m^{-2} day^{-1}, with clear maxima at high altitude. The combined deposition of SO_2 and halogenated acids is equivalent to H^+ fluxes of 1-30 mg m^{-2} day^{-1}, up to 10 times larger than observed deposition worldwide (Delmelle *et al.*, 2001). Parnell (1986) found that continuous volcanogenic acid inputs have decreased

the pH and cation exchange capacity (CEC) of the Masaya Andosols downwind.

The area surveyed has a tropical climate, with a mean annual rainfall of 1379 mm and a mean annual air temperature of 26.3 °C (UNA & ISRIC, 1994). The rainfall pattern is strongly seasonal: the rainy season lasts from May to October and accounts for 90% of the annual precipitation; the dry season (November-March) has a water deficit (P-ETP) ranging between 72 and 239 mm (Figure 2.11; UNA & ISRIC, 1994). The soil moisture regime is ustic (Soil Survey Staff, 1999).

The soil distribution pattern downwind of the volcano reflects both the age of the parent rock and distance from the source of the ash. According to a previous soil survey (Ministerio de Agricultura y Gonderia, 1971), the soils pertain to a Vitrand-Ustand-Ustoll sequence in the Soil Taxonomy (Soil Survey Staff, 1999; Figure 3.1), i.e. Vitric Andosol-Eutric Andosol-Chernozem in the WRB system (ISSS, 1998).

The area surveyed is covered with a thick succession of Holocene basaltic ash deposits erupted from the Masaya volcano (Parnell, 1986; Walker *et al.*, 1993). Table 3.1 lists a representative chemical composition of the volcanic products. A noteworthy feature of Masaya is the lack of temporal (> 30 000 years) and spatial variations in the chemistry of its tephra (Walker *et al.*, 1993). In addition, the basaltic rock is characterised by a large content of FeO (11.0-12.7 %) and small concentration of Al_2O_3 (15.6-16.8 %). Calcium dominates the alkali and alkaline-earth elements, followed by Mg, Na and K (Table 3.1).

Table 3.1: Chemical analysis of fresh pyroclasts, Vitric Andosol area (Walker *et al.*, 1993).

Compound	/%
SiO_2	50.50
Al_2O_3	16.30
FeO	11.40
TiO_2	1.05
CaO	10.00
MgO	3.75
K_2O	1.14
Na_2O	2.83
MnO	0.22
P_2O_5	0.25
TRB*	801 $cmol_c\ kg^{-1}$

*Herbillon (1986)

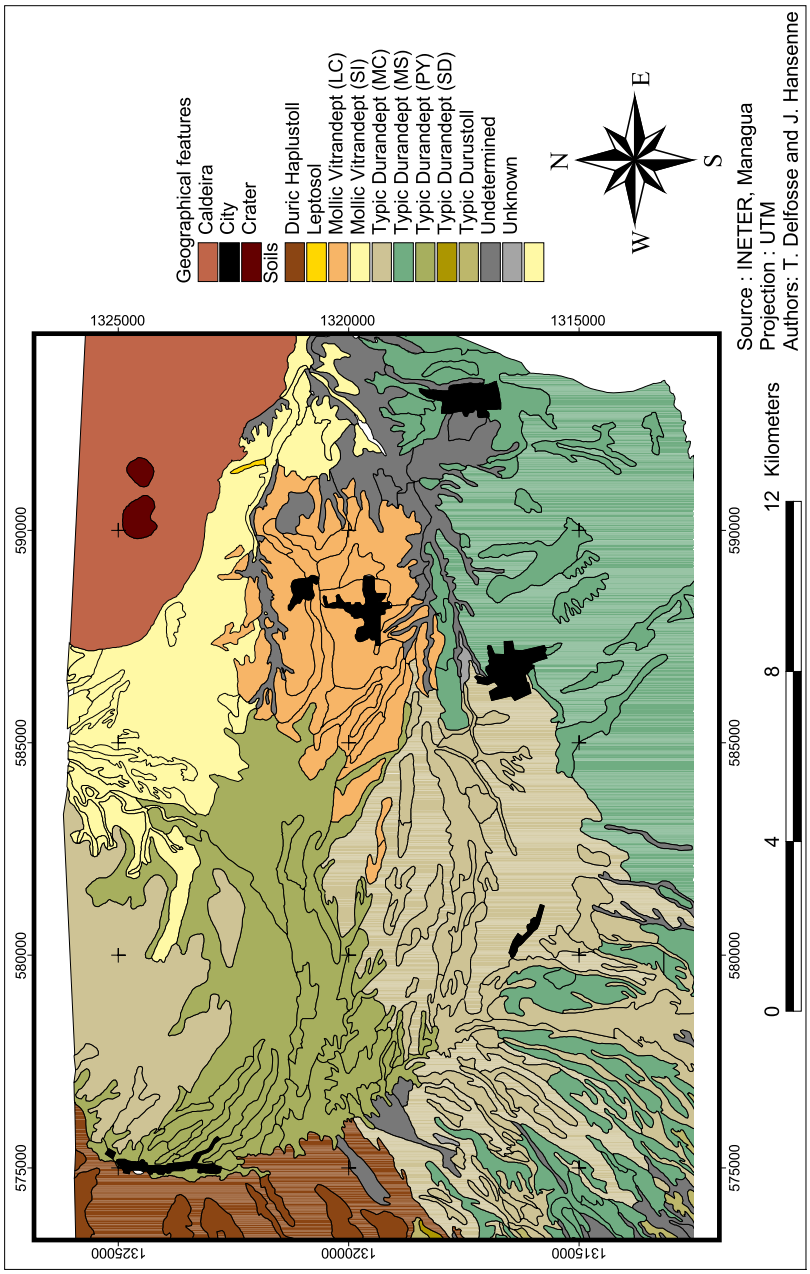

Figure 3.1: Soil map of the Masaya area. The San Ignacio (SI) series corresponds to the Vitric series, whereas the Pacaya (PY) and San Marcos (MC) series correspond to the Eutric series. Map adapted from Ministerio de Agricultura y Gonderia (1971).

3.3 Materials and methods

As can be seen on Figure 3.1, various soil series mantle the Masaya area. We selected the soil series most affected by the volcanic gas plume and studied ten soil profiles along two homogeneous and contrasting transects roughly perpendicular to the main plume direction (Figure 3.2). Transect 1 is on the Masaya caldera ridge 5 km from the active crater and comprises five Vitric Andosol profiles from the San Ignacio series (VI-2, 4, 6, 7 and 9; Figures 3.1, 3.2 and 3.3). Transect 2 is 15 km from the volcano in the Llano Pacaya area and consists of five Eutric Andosol profiles from the Pacaya and San Marcos series (EU-2, 4, 5, 6 and 9; Figures 3.1, 3.2 and 3.3).

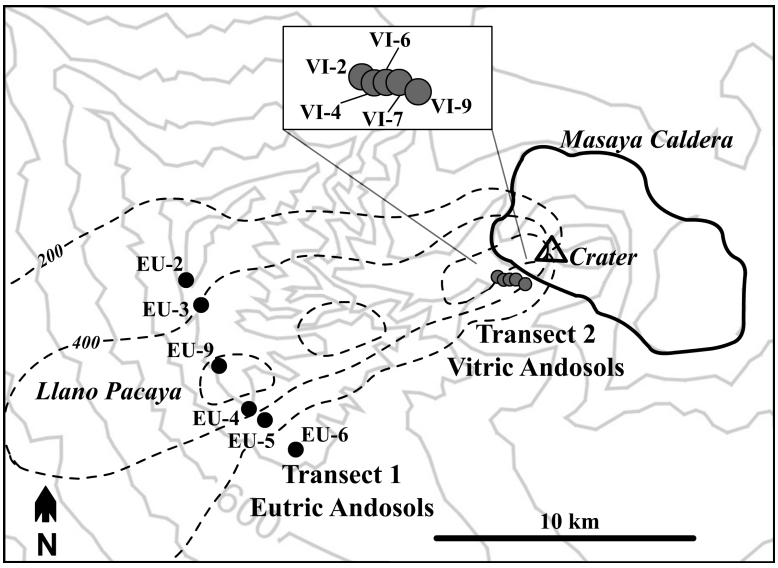

Figure 3.2: Map showing the locations of the Vitric (VI) and Eutric (EU) soil sites studied in the vicinity of the Masaya volcano. The dotted lines represent the sulphation rate (mg SO_2 m^{-2} day^{-1}) contour map adapted from Delmelle *et al.* (2001). The ellipse and the triangle sketch Masaya's caldera rim and degassing crater, respectively.

Data on SO_2 dry deposition (Delmelle *et al.*, 2001) indicate that the sites closest to the volcano (Vitric Andosols) receive more elevated acid inputs than the sites located further downwind (Eutric Andosols), although fumigation of the highlands also generates secondary maxima at a distance of 15 km from the volcano. On each transect, one site (EU6 and VI9 on eutric and Vitric transect, respectively) was chosen in a zone less affected by the volcanic plume on the basis of ambient SO_2 concentrations, SO_2 dry deposition rates and vegetation status (Delmelle

et al., 2001; 2002). A brief description of the sampling sites and ranges of dry SO_2 inputs is given in Table 3.2.

Table 3.2: Description, vegetation scale index (VSI) and SO_2 dry deposition data for each sampling site.

Profile	†Dry deposition /mmol SO_2 m^{-2} day^{-1}	‡VSI
Vitric transect		
VI-9	no data	II
VI-7	7.0±0.4	III
VI-6	7.4±0.4	III
VI-4	8.2±0.4	III
VI-2	9.0±0.4	III
Eutric transect		
EU-6	1.6±0.4	II
EU-5	3.9±0.4	II-III
EU-4	6.6±0.4	III
EU-9	9.0±0.4	III
EU-2	5.1±0.4	III

†SO_2 dry deposition rates from Delmelle *et al.* (2001)
‡ I No visible damage;
II observable leaf injury to trees and shrubs;
III vegetation is largely eliminated and consists mostly of a gas-tolerant weedy grass composite (see Delmelle *et al.*, 2002)

The soil profiles were dug to 100 cm and described according to the FAO standard guidelines. Since most of the acid neutralisation and S retention processes occur in the topsoil, we used the first 30-40 cm of each soil profile for chemical characterisation. Undisturbed soil cores were collected for bulk density measurement at a soil moisture content set at a matric tension of -33 kPa.

Laboratory analyses were carried out on <2 mm air-dried samples. Soil pH was measured in H_2O and in 1 M KCl with 1 g soil in 5 ml solution. Carbon content was determined according to the method of Walkley & Black (1934). Cation exchange capacity (CEC) and the content of exchangeable bases were determined according to Hendershot & Duquette (1986) for mineral horizon samples. Briefly, 3 g (Vitric) and 1 g (Eutric) of soil sample were shaken in batches with 20 ml of an unbuffered 0.1 M $BaCl_2$ solution for 2 hours. After centrifuging and filtration, the solution was analysed for cations by Inductively Coupled Plasma-Atomic Emission Spectrometry (ICP-AES). Three centrifuge-washing steps with 20 ml of 0.025 M $BaCl_2$, and four with 20 ml of 0.5 M $MgCl_2$, completed the procedure for CEC measurement. The last four supernatant solutions were saved for Ba analysis to determine the CEC.

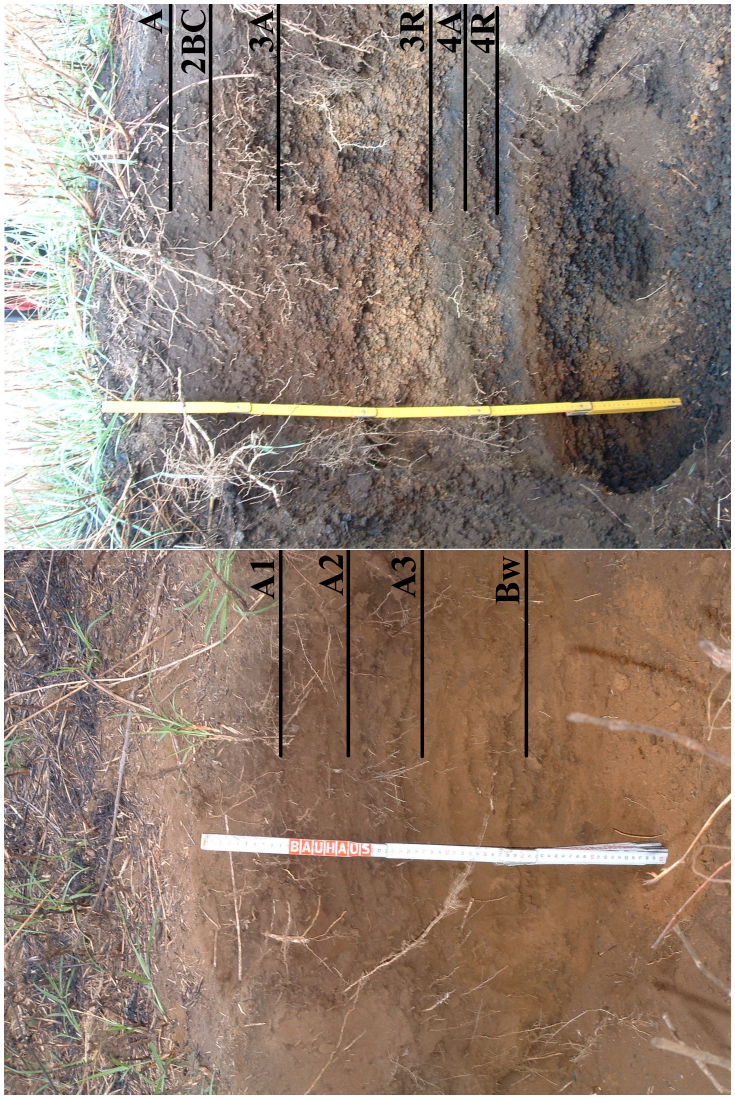

Figure 3.3: VI2 (right) and EU5 (left) profiles. These profiles are representative of the Vitric and Eutric Andosol series, respectively.

Phosphorous-retention was determined by the method of Blakemore *et al.* (1987).

Dark oxalate-extractable (o), dithionite citrate bicarbonate-extractable (DCB) (d) and pyrophosphate-extractable (p) contents of Si, Al and Fe were determined by the methods compiled in Dahlgren (1994). Except for sulphur, elemental analyses were carried out after Li-metaborate+Li-tetraborate fusion (Chao & Sanzolone, 1992). A crushed sample of 100 mg was melted at 1000 °C for 5 minutes in a graphite crucible in the presence of 0.4 g Li-tetraborate and 1.6 g Li-metaborate. The cooled melt was dissolved in 200 ml of 2 M HNO_3 under magnetic agitation at 90-100 °C and analysed by ICP-AES. Loss on ignition was measured at 950 °C. In order to determine the total S content in the soil, 200 mg of sample were heated in a vitrified graphite crucible in the presence of 1 g NaOH and 2 g Na_2O_2. The melt was dissolved in 30 ml HCl and total S was measured by ICP-AES.

The specific surface, i.e. surface area per mass (S_m), of the soil samples was measured by the ethylene glycol monoethyl ether (EGME) method (Carter *et al.*, 1965). Hygroscopic water removal was achieved under vacuum in the presence of anhydrous P_2O_5, and the Camp–Berteau Montmorillonite (810 $m^2\ g^{-1}$) was used as internal standard.

3.4 Results

3.4.1 Morphology

The major morphological properties of the Vitric and Eutric Andosols profiles are summarised in Annexes 1a and 1b, respectively. Each soil series showed a remarkably uniform profile development. Within the first meter, the Vitric Andosols are developed in six successive ash-fall deposits. The soils contain fresh pyroclastic fragments. They derive from unconsolidated pyroclastic rock (ash, lapilli, scoriae), and drained rapidly. The Eutric Andosols are developed in weathered ash. The soils exhibit an A-AB-Bw development profile. They have a loam to clay loam field texture and exhibit smeariness at depth. They are freely drained. The first 40 cm of the profile appears to derive from a single ash-fall.

3.4.2 Physico-chemical properties

The organic C content, CEC, sum of exchangeable bases (Σ), S_m and pH of the soil samples are listed in Table 3.3. For some horizons, bulk density and P-retention are also reported. The CEC, carbon content and pH in water are generally less in the Vitric Andosols (3.9-19.7 $cmol_c\ kg^{-1}$,

8-35 g kg^{-1}, 3.8-6.6, respectively) than in the Eutric soils (16.5-69.6 $cmol_c$ kg^{-1}, 33-91 g kg^{-1}, 5.2-7.6, respectively). The Eutric Andosols display systematically larger S_m (144-308 m^2 g^{-1}) than the Vitric Andosols (20-119 m^2 g^{-1}).

The bulk densities of the selected soil horizons range from 0.79 to 0.90 g cm^{-3}. The P-retention in the Eutric Andosols exceeds 70% except for one A horizon (EU6 A1: 68 %, Table 3.3). In the Vitric Andosols, P-retention ranges from 51 to 86 %.

3.4.3 Total element content and selective extractions

Tables 3.4 and 3.5 list the total element contents. In Table 3.4 they are given as oxides. Table 3.5 reports the total contents of alkali and alkaline-earth elements expressed in $cmol_c$ kg^{-1}. Silicon oxide content is less in Eutric (25-46 %) than in Vitric Andosols (43-51 %). Aluminium and Fe oxide contents are similar in the two soil types: the average total contents are ∼16 % and ∼13 % for Al_2O_3 and Fe_2O_3, respectively. The content of SO_3 in the Vitric and Eutric Andosols ranges from 0.17 to 0.55 % and from 0.22 to 1.37 %, respectively. The determination of loss on ignition allows the closure of the balance, which ranges from 99.7 to 100.6 %.

Table 3.6 lists the contents of Al_o, Si_o, Fe_o, Al_p and Fe_d. Oxalate-extractable Si, Al, Fe and Fe_d contents are always greater in the Eutric than in the Vitric Andosols, except in the buried 3A Vitric horizons. The relative importance of iron oxide can be assessed through Fe_d:Fe_t. This ratio is always smaller in the Vitric (0.1-0.3) than in the Eutric Andosols (0.3-0.9). Similarly, the sum [Al_o+ $\frac{1}{2}$ Fe_o] is smaller in the Vitric (0.7-4.3 %) than in the Eutric soils series (3.1-11.6 %). The Total Reserve in Bases (TRB) is the sum of total Na, K, Ca and Mg and estimates the content of weatherable minerals in mineral soils (Herbillon, 1986). The TRB of unweathered tephra is 801 $cmol_c$ kg^{-1} (Table 3.1), whereas the TRB in the Vitric Andosols is in the range 432-629 $cmol_c$ kg^{-1}, which is significantly larger than in the Eutric Andosols (164-418 $cmol_c$ kg^{-1}; Table 3.5). The 3A and 3AB horizons of the Vitric Andosols always display smaller TRB values than the more superficial horizons, as a result of longer weathering (buried weathered horizons). The lack of variation in the TRB values of the Eutric horizons supports the morphological observations that a unique deposit of ash constitutes the parent material of the first few decimetres of the soil profile. Calcium represents about 53 % of the TRB in the unweathered parent material (Figure 3.4) and is also the dominant TRB cation (50 %) in the Vitric soils (Figure 3.4). The contribution of Ca to TRB is reduced to 40 %

Table 3.3: Major properties of the various soil horizons. pH, carbon content, CEC and sum of exchangeable cations (Σ), Specific Surface (S_m) and P retention (P ret.) of the soil profiles.

Prof.	Horiz.	Depth /cm	pH (H_2O)	pH (KCl)	Org. C /g kg^{-1}	CEC /$cmol_c$ kg^{-1}	Σ	Sm /m^2 g^{-1}	P ret. /%
VI2	A	0-9	4.4	4.3	21	4.9	0.4	29	-
	2BC	9-14	4.5	4.4	10	4.4	0.3	77	-
	3A	14-24	4.9	4.3	20	7.8	0.9	83	-
VI4	A	0-7	3.8	3.6	24	6.8	1.0	29	-
	2BC	7-13	4.6	4.5	12	4.9	0.3	30	-
	3A	13-24	4.6	4.4	32	10.6	1.5	118	-
VI6	A	0-6	3.8	3.7	23	6.7	1.4	34	58
	2BC	6-14	4.8	4.5	9	3.9	0.3	20	53
	3A	14-20	5.3	4.4	31	13.1	4.1	84	83
	3AB	20-29	6.1	4.9	35	19.7	13.8	95	86
VI7	A	0-7	4.6	4.3	20	5.5	-	29	-
	AB	7-17	5.5	4.6	12	5.3	0.7	32	-
	2BC	17-22	5.2	4.6	8	4.3	0.6	26	-
	3AB	22-28	6.1	4.9	23	12.8	8.5	50	-
VI9	A	0-6	5.3	4.5	28	11.5	7.0	64	51
	2BC	6-15	6.1	4.9	16	9.8	6.4	44	55
	3A	15-21	6.6	5.3	35	11.4	22.6	119	78
EU2	A1	0-7	5.5	4.8	89	33.5	24.6	194	-
	A2	7-16	5.3	4.6	81	28.4	11.3	215	-
	A3	16-22	5.2	4.7	91	23.7	9.9	223	-
	AB	22-29	5.2	4.7	88	24.3	3.5	235	-
	Bw	29-39	5.3	5.0	58	21.8	27.9	308	-
EU9	A1	0-6	5.9	5.2	59	33.3	29.5	144	-
	A2	6-24	5.7	4.7	47	21.5	11.6	163	-
	AB	24-33	5.5	4.8	45	21.0	9.2	231	-
EU4	A1	0-6	5.6	4.8	54	24.7	15.1	146	94
	A2	6-18	5.9	4.8	52	25.5	15.7	155	92
	AB	18-24	5.6	4.7	38	17.9	7.5	176	94
	BA	24-37	5.7	4.8	37	16.5	6.5	193	94
EU5	A1	0-5	6.7	5.5	67	41.4	38.7	161	-
	A2	5-16	6.9	5.6	51	36.9	33.4	170	-
	A3	16-27	7.0	5.6	52	36.8	32.8	155	-
	Bw1	27-39	6.9	5.6	40	25.5	15.0	246	-
EU6	A1	0-6	7.2	6.4	67	69.6	77.7	147	68
	A2	6-19	7.6	6.3	52	53.0	65.7	166	78
	AB	19-29	7.4	6.0	43	41.1	35.4	186	84
	BA	29-40	7.1	5.8	33	30.5	24.7	222	88

in the Eutric Andosols, while Mg is the dominant cation, accounting for 50 % of the TRB. Sodium and K contribute less to the TRB and account, respectively, for ∼12 % and ∼4 % in the Eutric and Vitric soils, respectively.

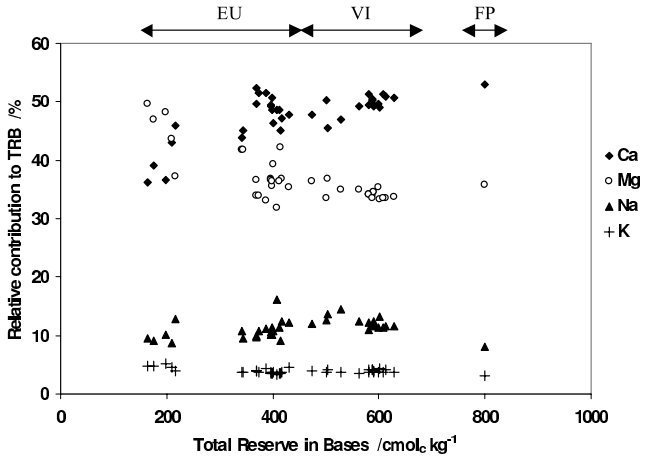

Figure 3.4: Relative contribution of alkali and alkaline earth cations to TRB in the Eutric and Vitric Andosols studied and in fresh pyroclasts (FP; Table 3.1; Walker *et al.*, 1993).

3.5 Discussion

The combination of $[Al_o + \frac{1}{2} Fe_o] > 2\%$, P-retention $> 70\%$ and bulk density < 0.9 g cm^{-3} (not shown) and base saturation $> 50\%$ in the first 30 cm (Tables 3.3 and 3.6) leads to classify the EU soils as Eutric Andosols. Having $[Al_o + \frac{1}{2} Fe_o] > 0.4\%$, P-retention $> 25\%$ (Tables 3.3 and 3.6) and being rich in volcanic glass (Parnell, 1986), VI soils are Vitric Andosols in the WRB system.

3.5.1 Soil weathering stage and implications for soil properties

Weathering of volcanic ash of similar composition led to decrease the total content of alkali and alkaline-earth cations (TRB) and increased the release of free iron, thus revealing a more advanced stage of weathering in Eutric than in Vitric Andosols. Convincingly, TRB and Fe_d:Fe_t are strongly and negatively correlated (r = -0.91) (Figure 3.5).

Oxalate-extractable Si, Al and Fe contents reflect the abundance of Al, Si and Fe released by pyroclast weathering and incorporated into

Table 3.4: Total elemental contents given as oxides and loss on ignition (LOI).

Prof.	Horz.	SiO_2	Al_2O_3	Fe_2O_3	TiO_2	CaO	MgO	K_2O	Na_2O	MnO_2	P_2O_5	SO_3	LOI
		/%											
VI2	A	48.36	14.63	14.91	1.03	8.17	4.10	1.03	2.29	0.20	0.30	0.30	4.94
	2BC	48.62	15.51	14.29	1.03	8.33	4.26	1.08	2.10	0.21	0.31	0.41	4.26
	3A	47.17	16.29	12.85	1.00	6.96	3.72	0.91	2.38	0.22	0.33	0.55	8.09
VI4	A	47.92	14.42	13.57	1.02	8.30	4.04	1.13	2.12	0.19	0.32	0.40	6.96
	2BC	49.24	15.61	13.28	1.05	8.19	4.11	1.09	2.20	0.21	0.32	0.27	4.61
	3A	43.14	18.26	11.53	1.00	5.79	3.07	0.93	1.64	0.18	0.36	0.50	13.99
VI6	A	49.18	14.53	12.46	1.05	8.07	4.01	1.14	2.18	0.16	0.30	0.32	6.88
	2BC	50.40	16.63	11.78	1.11	8.75	4.13	1.18	2.19	0.18	0.29	0.29	3.34
	3A	45.24	15.29	13.43	1.02	6.43	3.73	0.96	2.12	0.24	0.36	0.54	11.01
	3AB	43.48	14.66	14.47	1.02	6.36	3.48	0.87	1.77	0.22	0.39	0.50	13.21
VI7	A	50.08	15.02	12.18	1.05	8.28	4.05	1.21	2.46	0.20	0.32	0.25	5.11
	AB	49.99	16.31	11.87	1.08	8.75	4.11	1.09	2.14	0.17	0.28	0.34	4.20
	2BC	50.70	16.12	12.07	1.08	8.93	4.28	1.13	2.27	0.17	0.28	0.21	2.87
	3AB	47.77	15.32	12.39	1.01	7.76	3.96	0.95	2.15	0.18	0.32	0.22	8.00
VI9	A	48.82	15.16	11.84	1.03	8.38	3.99	1.01	1.97	0.17	0.41	0.21	7.18
	2BC	50.01	15.94	11.55	1.05	8.33	3.98	1.13	2.16	0.18	0.34	0.17	5.01
	3A	44.60	15.00	13.42	0.94	7.06	3.39	0.88	1.96	0.22	0.45	0.28	11.92
EU2	A1	28.07	15.02	14.77	1.09	2.80	1.63	0.41	0.86	0.24	0.33	0.64	34.79
	A2	31.66	17.40	11.79	1.31	2.53	1.84	0.45	0.56	0.27	0.36	0.59	31.69
	A3	24.90	17.80	17.51	1.35	1.93	1.66	0.40	0.50	0.33	0.32	1.37	32.10
	AB	25.04	20.08	16.37	1.50	1.66	1.63	0.37	0.48	0.35	0.34	1.24	31.17
	Bw	26.76	22.66	14.46	1.63	2.04	1.93	0.48	0.62	0.30	0.29	1.09	28.23
EU9	A1	40.38	13.65	14.12	0.99	5.40	2.55	0.66	1.25	0.21	0.40	0.38	20.15
	A2	39.86	15.49	15.92	1.12	5.46	2.93	0.64	1.42	0.26	0.37	0.39	16.27
	AB	40.23	17.66	12.46	1.32	4.33	2.89	0.60	1.01	0.29	0.37	0.44	18.67
EU4	A1	40.87	15.79	11.47	1.18	5.52	3.10	0.71	1.61	0.25	0.36	0.34	19.10
	A2	39.66	15.13	13.90	1.10	5.13	2.72	0.66	1.12	0.24	0.33	0.36	19.48
	AB	38.36	17.40	15.59	1.26	5.23	3.18	0.69	1.34	0.26	0.28	0.47	16.41
	BA	42.28	18.27	11.47	1.38	5.25	3.53	0.69	1.17	0.29	0.31	0.46	15.30
EU5	A1	37.83	14.51	12.68	1.01	5.55	2.61	0.63	2.05	0.21	0.36	0.32	22.44
	A2	42.28	16.08	10.47	1.16	5.46	2.93	0.66	1.28	0.26	0.38	0.29	18.69
	A3	39.75	16.02	14.06	1.13	5.67	2.85	0.67	1.25	0.25	0.31	0.26	17.89
	Bw1	36.44	20.53	12.91	1.50	4.19	2.86	0.58	1.14	0.30	0.33	0.59	19.02
EU6	A1	42.13	13.23	8.22	0.97	5.43	2.53	0.69	1.10	0.22	0.51	0.51	24.91
	A2	45.45	14.74	9.73	1.05	5.60	2.59	0.78	1.35	0.24	0.36	0.29	18.02
	AB	46.04	16.22	9.94	1.20	5.49	2.93	0.70	1.25	0.26	0.37	0.22	15.07
	BA	42.63	17.50	12.56	1.30	5.62	3.02	0.67	1.46	0.26	0.31	0.25	14.60

Table 3.5: Total alkali and alkaline-earth elemental contents, total reserve in bases (TRB), Al, Fe, S and P amounts contributing to acid neutralising capacity (ANC_S) according to Equation 3.2, and ANC_S.

Prof.	Horz.	Ca^{2+}	Mg^{2+}	K^+	Na^+	TRB	Al	Fe	S	P	ANC_S
		/cmol$_c$ kg^{-1}									
VI2	A	292	204	22	73	591	860	515	8	13	1946
	2BC	298	211	23	68	600	912	484	10	13	1973
	3A	248	185	19	77	530	958	382	14	14	1842
VI4	A	296	200	24	69	589	848	467	10	13	1881
	2BC	293	204	23	71	591	918	435	7	13	1924
	3A	207	152	20	53	432	1074	355	12	15	1833
VI6	A	288	199	24	70	582	855	424	8	13	1840
	2BC	313	205	25	70	613	978	407	7	12	1978
	3A	230	185	20	68	503	899	368	14	15	1742
	3AB	227	173	18	57	475	862	376	12	16	1685
VI7	A	296	201	26	79	602	883	411	6	13	1876
	AB	312	204	23	69	609	959	372	9	12	1919
	2BC	319	212	24	74	629	948	424	5	12	1983
	3AB	277	197	20	69	563	901	418	6	14	1863
VI9	A	299	198	21	64	582	891	399	5	17	1850
	2BC	298	198	24	69	589	937	384	4	14	1892
	3A	252	168	19	63	502	882	376	7	19	1734
EU2	A1	100	81	9	27	217	883	252	16	14	1322
	A2	90	91	9	19	209	1023	114	15	15	1317
	A3	69	82	9	16	176	1047	268	34	14	1442
	AB	59	81	8	16	164	1181	150	31	14	1450
	Bw	73	96	10	20	199	1333	81	27	12	1573
EU9	A1	193	126	14	40	373	803	352	9	17	1502
	A2	195	145	14	46	400	911	397	10	16	1683
	AB	155	143	13	32	343	1038	189	11	16	1543
EU4	A1	197	154	15	52	418	929	223	9	15	1545
	A2	183	135	14	36	368	890	319	9	14	1554
	AB	187	158	15	42	402	1023	351	12	12	1753
	BA	188	175	15	37	415	1074	195	11	13	1660
EU5	A1	198	129	13	66	407	853	277	8	15	1514
	A2	195	146	14	41	396	946	173	7	16	1492
	A3	202	141	14	41	398	942	296	6	13	1617
	Bw1	150	142	12	37	341	1207	138	15	14	1657
EU6	A1	194	126	15	35	370	778	143	13	21	1257
	A2	200	128	16	44	388	867	169	7	15	1401
	AB	196	146	15	40	397	954	148	6	16	1477
	BA	201	150	14	47	412	1029	203	6	14	1624

Table 3.6: Si, Al and Fe contents in oxalate (o), dithionite (d) and pyrophosphate (p) extracts.

Profile	Horiz.	Si_o	Al_o	Fe_o	Al_p	Fe_d	Fe_d:Fe_t	$Al_o+\frac{1}{2}Fe_o$
		/g kg^{-1}						/%
VI2	A	3.1	6.2	8.3	1.8	8.4	0.1	1.0
	2BC	4.1	7.5	7.6	1.8	9.8	0.1	1.1
	3A	5.3	9.6	8.5	2.7	18.7	0.2	1.4
VI4	A	1.8	3.9	6.4	1.6	8.0	0.1	0.7
	2BC	3.6	7.0	7.1	2.1	11.9	0.1	1.1
	3A	19.1	32.6	21.6	4.3	14.6	0.2	4.3
VI6	A	1.8	3.9	8.2	1.8	8.3	0.1	0.8
	2BC	3.1	6.0	5.8	1.7	6.6	0.1	0.9
	3A	8.1	15.2	15.1	3.8	25.4	0.3	2.3
	3AB	12.5	21.3	19.6	3.7	31.2	0.3	3.1
VI7	A	2.8	5.8	8.4	2.1	8.8	0.1	1.0
	AB	3.3	6.4	7.7	1.9	13.9	0.2	1.0
	2BC	2.7	4.9	5.6	1.4	5.5	0.1	0.8
	3AB	5.6	9.7	8.5	2.3	8.8	0.1	1.4
VI9	A	2.6	4.7	9.6	1.7	8.6	0.1	1.0
	2BC	3.4	6.2	10.1	1.7	9.3	0.1	1.1
	3A	15.5	24.7	25.5	2.7	23.9	0.3	3.7
EU2	A1	23.3	49.9	37.0	11.1	56.5	0.5	6.8
	A2	25.0	55.2	41.8	11.8	61.3	0.7	7.6
	A3	29.7	68.4	52.4	11.9	72.6	0.6	9.5
	AB	34.9	76.6	57.5	10.0	86.5	0.8	10.5
	Bw	41.5	83.6	65.4	7.0	86.0	0.9	11.6
EU9	A1	16.3	28.9	25.9	4.4	33.2	0.3	4.2
	A2	19.0	34.5	29.2	5.5	37.5	0.3	4.9
	AB	29.4	48.4	36.9	4.6	52.1	0.6	6.7
EU4	A1	18.9	31.5	28.1	4.9	38.8	0.5	4.6
	A2	18.1	32.3	26.7	5.8	37.9	0.4	4.6
	AB	24.0	40.6	33.5	4.8	43.7	0.4	5.7
	BA	24.3	38.8	31.5	4.3	44.0	0.5	5.4
EU5	A1	17.3	29.0	23.7	3.4	37.2	0.4	4.1
	A2	19.4	33.4	27.1	3.9	41.0	0.6	4.7
	A3	22.1	35.3	27.8	3.7	43.2	0.4	4.9
	Bw1	37.1	61.0	45.2	3.5	64.6	0.7	8.4
EU6	A1	13.6	21.0	19.9	2.0	30.8	0.5	3.1
	A2	15.1	23.8	21.9	2.5	36.6	0.5	3.5
	AB	20.8	31.9	31.0	2.6	42.0	0.6	4.7
	BA	31.0	43.2	37.5	2.5	50.1	0.6	6.2

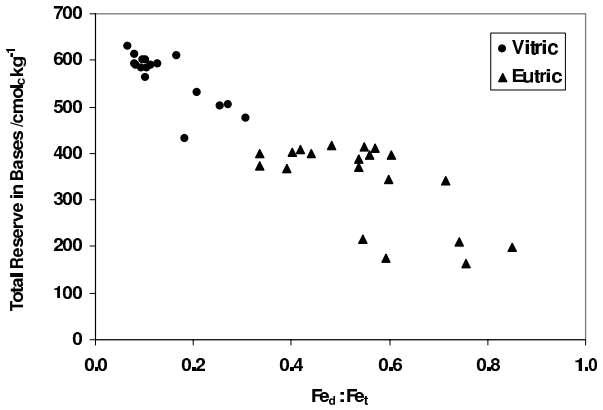

Figure 3.5: Relationship between TRB and Fe_d:Fe_t in the Andosols studied.

secondary constituents. As shown in Figure 3.6, Si_o and TRB are negatively correlated (r = -0.89). Strong negative correlations are also found between TRB and Al_o (r = -0.94), and TRB and Fe_o (r = -0.93) (not illustrated). This supports the enhanced formation of short-range ordered minerals (allophane and ferrihydrite) in the more weathered soils. Allophane content (Parfitt & Wilson, 1985) and ferrihydrite content (Mizota & van Reeuwijk, 1989), increased from Vitric (1-13 %, 1-4 %, respectively) to Eutric Andosols (10-29 %, 3-11 %, respectively). The increase in mineral content is associated with a large CEC increase from 3.9-19.7 $cmol_c\ kg^{-1}$ in Vitric Andosols to 16.5-69.6 $cmol_c\ kg^{-1}$ in Eutric Andosols (Table 3.3).

The observed decrease in TRB is accompanied by a significant decrease in total soil SiO_2 concentration (Figure 3.7, r = 0.95). In contrast, total Fe_2O_3 and Al_2O_3 concentrations do not vary. This illustrates the importance of the desilicification process in the weathering of volcanic glass and the concomitant relative accumulation of Al and Fe. Silicon released by weathering was partially incorporated into allophanic minerals and lost by drainage, whereas Al and Fe accumulated into allophanic constituents and ferrihydrite, respectively.

Formation of secondary short-range ordered minerals during pyroclast weathering resulted in increased S_m, which is strongly and negatively correlated with TRB (r = -0.92), and strongly and positively correlated with Si_o (Figure 3.8), Al_o and Fe_o contents (r = 0.97, 0.95 and 0.94, respectively). From Figure 3.8, we calculated the following linear regression:

$$S_m = 24 + 6.7\, Si_o, \tag{3.1}$$

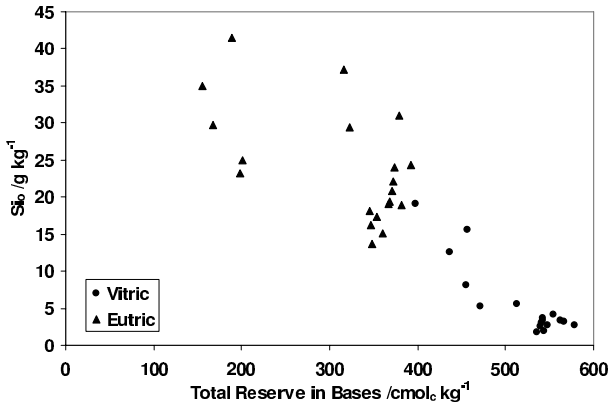

Figure 3.6: Relationship between Si_o content and TRB in the Andosols under study.

in which S_m is in $m^2\ g^{-1}$ and Si_o is in g kg^{-1}. The combination of Equation (3.1) with the expression relating allophane content to Si_o (Parfitt & Wilson, 1985) leads to an estimate of S_m of $\sim$10 $m^2\ g^{-1}$ per % of allophane, i.e. 1000 $m^2\ g^{-1}$ allophane. This agrees well with previous measurements of S_m in allophanic constituents by EGME (700-1100 $m^2\ g^{-1}$; Shoji *et al.*, 1993; Harsh *et al.*, 2002).

3.5.2 Soil pH and exchangeable base cations

The Vitric and Eutric soil samples have pH (H_2O) values ranging from 3.8 to 6.6, and from 5.2 to 7.6, respectively (Table 3.3). On each transect, soil slurry pHs are consistently lower at any depth for sites directly exposed to the volcanic acid emissions as compared to the site located on the plume margin (Table 3.3, Figure 3.9). These results suggest an influence of the volcanogenic acid inputs on soil pH, an effect previously reported by Parnell (1986) for four soil profiles collected from the Eutric area in 1981.

Since the Eutric soils are enriched in allophanes and organic matter as compared to the Vitric soils, they also have an enhanced cation exchange capacity, and consequently higher exchangeable base cation concentrations (Table 3.3). However, for soils with similar characteristics, exchangeable base cations are depressed in the most acid-impacted sites and at every depths through the profile (Table 3.3, Figure 3.9), again suggesting a chemical response to acidification of the Andosols. Loss of exchangeable base cations is associated to a decrease in the negative

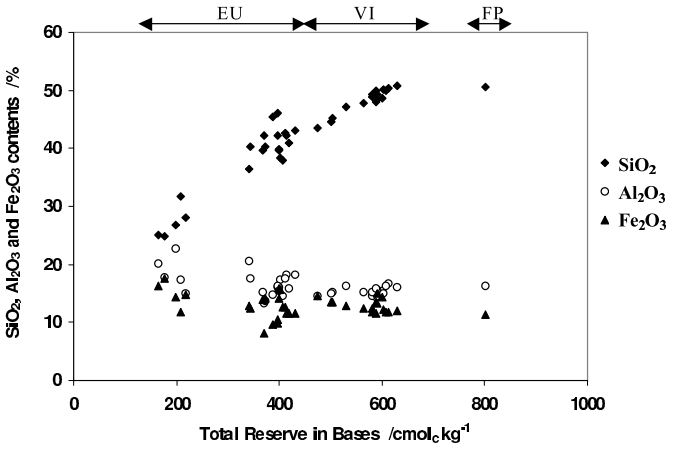

Figure 3.7: Relationship between TRB and total SiO_2, Al_2O_3 and Fe_2O_3 contents in the Eutric and Vitric Andosols studied and in fresh pyroclasts (FP; Table 3.1; Walker *et al.*, 1993).

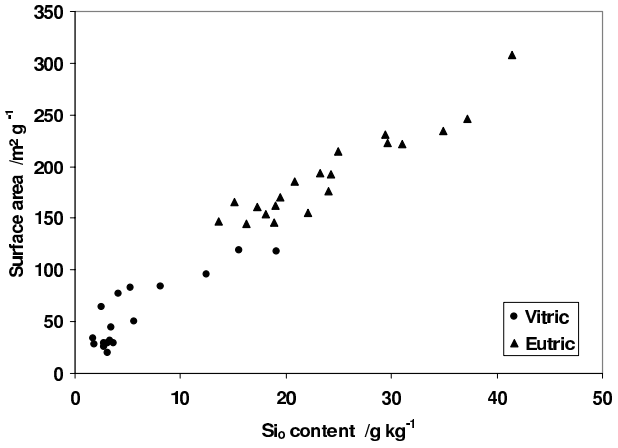

Figure 3.8: Relationship between specific surface (S_m) and Si_o content in the Andosols under study.

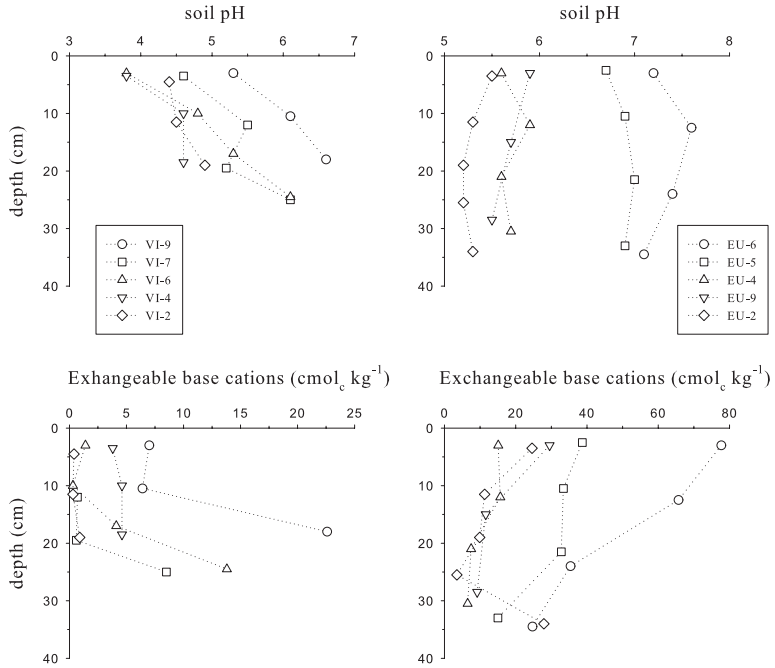

Figure 3.9: Graph of pH and exchangeable base cation concentration versus depth in the Vitric and Eutric Andosol profiles.

charges of the soil constituents which results from the soil pH decrease (Parnell, 1986; Dahlgren *et al.*, 1990). The relationship between exchangeable base cation concentrations and pH is clearly reflected within the Eutric Andosol group; EU-6 (and EU-5) have significantly higher pH values than the other sites and their base contents are also higher, despite comparatively low allophane contents.

3.5.3 Sulphur storage and net acidification of soils

Masaya Andosols continuously exposed to SO_2 contain 680-5470 mg S kg^{-1}soil, more than typical contents reported in the literature. Soils receiving acid rain generally show total S contents from 100 to 700 mg S kg^{-1} (e.g. Mayer *et al.*, 2001), whereas soils affected by marine aerosol or by fumaroles may contain similar amounts of S than Masaya Andosols (Hue *et al.*, 1990; Takamatsu *et al.*, 1992).

In order to assess the contribution of total sulphur content to the variation within our soil samples, we carried out a principal component analysis (PCA) using the data set listed in Tables 3.3 and 3.5 (37 exper-

imental points). We included the following standardised variables TRB, Fe_d:Fe_t ratio, pH, CEC, carbon content (C), Si_o and SO_3, and used the correlation matrix. The results of the PCA are illustrated in Figure 3.10. The eigenvalues are listed in Table 3.7. The first and second principal components (PC) contribute to 67 % and 21 % of the total variance, respectively. The first PC contrasts TRB with Si_o content, and TRB versus Fe_d:Fe_t ratio, thereby discriminating soils according to weathering stage. The second PC contrasts pH and CEC with SO_3. Largest total S contents are thus related to the most acid horizons with smaller CEC. The sulphur-impacted sites tend to contain more SO_3 than less impacted sites (Table 3.4), indicating that long-term exposure to volcanic S has increased the total sulphur content of the soils downwind from the volcano. The second PC may thus distinguish soils that have received different deposition rates or with distinct S sorption capacities.

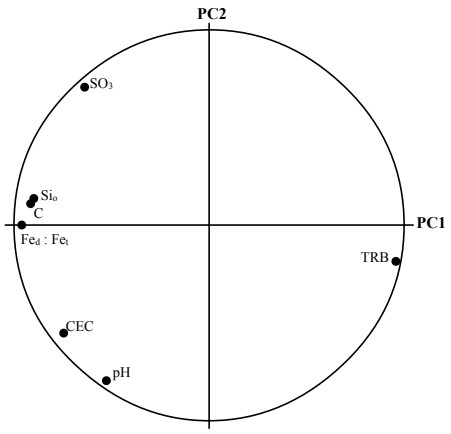

Figure 3.10: Plane projection of the correlations between the seven soil properties (standardised variables) and the principal component scores into unit circle in the plane of the first two components.

Acid loading and strong SO_3 accumulation may also affect the acid neutralising capacity of the solid phase of the soil (ANC_s). We used a modified expression of ANC ($_mANC_s$), taking into account SO_3 and P_2O_5 contents of soil. Allophane might not be stable at this pH (Harsh *et al.*, 2002), and total Al was thus taken into account, as follows:

$$_{m}ANC_{s\ (pH\ 3)} = [TRB]+6[Al_2O_{3t}]+6\{Fe_2O_{3t}-Fe_2O_{3d}\}-2[SO_3]-2[P_2O_5] \quad (3.2)$$

where [ ] denotes total molar concentration and { } is partial molar concentration in $cmol_c\ kg^{-1}$. The TRB is expressed as 2 [CaO + MgO + Na_2O + K_2O], and 6 {Fe_2O_{3t} - Fe_2O_{3d}} reflects the content of Fe_2O_3

in Fe-bearing silicates. On each transect, except for the more weathered EU-2 profile, the acid-impacted sites tend to have ANC_s values similar to those of less impacted sites (Table 3.5). Prolonged inputs of acid had negligible effects on mineral reserves compared with that on physico-chemical properties such as pH and CEC.

The difference in ANC_s between Vitric Andosols (1685-1983 $cmol_c$ kg^{-1}) and Eutric Andosols (1257-1753 $cmol_c$ kg^{-1}; Table 3.5) is attributed to differences in TRB values and Fe-bearing silicates content. The values of TRB in the Vitric Andosols are generally 200 $cmol_c$ kg^{-1} larger than in Eutric Andosols. The contribution of Fe to ANC_s is larger in Vitric Andosols (355-515 $cmol_c$ kg^{-1}) than in Eutric Andosols (81-397 $cmol_c$ kg^{-1}), whereas that of Al is similar in both soil types ($\sim$800 to $\sim$1100 $cmol_c$ kg^{-1}). The decrease in TRB and increase in free iron contents induced by weathering both lead to a decrease in ANC_s.

The contribution of SO_3 to ANC_s is fairly small. In the Vitric Andosols, SO_3 accounts for 4 to 14 $cmol_c$ kg^{-1} in ANC_s (Table 3.5), whereas in Eutric Andosols, it contributes more but still only 6 to 34 $cmol_c$ kg^{-1}. These results indicate that even with remarkably large soil sulphur content, the ANC_s of these Andosols is not significantly depleted.

At the pH of the Eutric soils (5.2-7.5), the dissolution of Fe and Al oxides is negligible, whereas in Vitric Andosols Fe and Al would not be leached out of the system. In our Andosols, ANC_s is thus influenced mostly by four pools: (i) exchangeable cations, (ii) non-exchangeable cations (mineral reserve), (iii) total SO_3 and (iv) total P_2O_5. The sum of these four pools constitutes the Total Reserve of Major Ions (TRMI).

In the Vitric Andosols, the stock of non-exchangeable cations (mineral reserve) largely dominates the TRMI (90.8-97.3 %; Table 3.8), whereas the contents of exchangeable cations, SO_3 and P_2O_5 contribute on average 0.8, 1.5 and 2.4 %, respectively. Mineral hydrolysis is thus the main process of proton consumption in Vitric Andosols. In the Eu-

Table 3.7: Eigenvalues of correlation matrix.

Order	Eigenvalue	Percentage	Acccumulated Percentage
1	4.714	67.34	67.34
2	1.503	21.47	88.81
3	0.439	6.27	95.08
4	0.186	2.66	97.73
5	0.103	1.47	99.20
6	0.044	0.63	99.83
7	0.011	0.16	100.00

Table 3.8: Total reserve of major ions (TRMI) given as means (minimum to maximum in parentheses) in Vitric and Eutric Andosols, and the relative contribution of exchangeable cation content, mineral reserve (i.e. TRB – exchangeable cation content), and total SO_3 and P_2O_5 content to TRMI.

	Vitric Andosol	**Eutric Andosol**
TRMI /$cmol_c$ kg^{-1}	586 (459-646)	368 (209-442)
Contribution to TRMI / %		
Exchangeable cations	0.8 (0.0–4.3)	6.7 (1.5–19.2)
Mineral reserve	95.3 (90.8–97.3)	84.6 (71.8–93.0)
SO_3	1.5 (0.7–2.7)	4.4 (1.3–15.3)
P_2O_5	2.4 (1.8–3.6)	4.3 (2.8–6.9)

tric Andosols, however, the contribution of mineral reserves to TRMI is smaller and accounts for 71.8 to 93.0 %. The contribution of the exchangeable cation content thus increases to 1.5-19.2 %, whereas total SO_3 and P_2O_5 contents account for 1.3-15.3 % and 2.8-6.9 % of TRMI, respectively. Acid neutralising processes in the Eutric soils may thus involve mineral weathering and ion exchange, either cation exchange with H^+ or sulphate adsorption and subsequent release of OH^- (e.g. Rajan, 1978).

Acid-buffering capacity is the ability of soil to resist pH change, and is measured over short times. Weathering of primary minerals is generally not significant in acid-buffering for times less than decades, whereas ion exchange and sorption readily contribute to pH-buffering because they are rapid (Bloom *et al.*, 2000). With their large content of allophane and ferrihydrite, Eutric Andosols thus show larger acid-buffering capacity than Vitric Andosols. This explains why pHs are smaller in Vitric (pH 3.8-6.5) than in Eutric Andosols (pH 5.2-7.5), despite larger ANC_s in the former than in the latter. This observation emphasises the importance of the acid-buffering capacity compared with mineral weathering of soils in reacting rapidly to acid deposition.

Eutric Andosols thus have a larger acid-buffering capacity but smaller ANC_s than Vitric Andosols because they have a much larger specific surface, linked to their large content of colloidal constituents (i.e. allophane and ferrihydrite). These constituents play a key role in regulating proton fluxes through cation exchange. Interestingly, they would also contribute to acid-buffering largely through anion exchange, which results in H^+ removal from soil solution, and reduces cation leaching. Sulphate sorption could therefore be a key process in acid-buffering in

the Eutric Andosols we studied. In addition, other processes such as sulphate immobilisation in organic matter or precipitation in aluminium-hydroxy sulphate minerals would also contribute to acid-buffering because they release OH^-, remove H^+ from solution or reduce base cation leaching. All these processes, however, contribute to store acidity as SO_3 within the solid phase, and thus deplete ANC_s because release of SO_3 leads to the production of sulphuric acid (van Breemen *et al.*, 1983). These considerations call for a comprehensive understanding of the fate of inorganic sulphate in these SO_2-impacted soils.

3.6 Conclusions

The Masaya area is endowed with Vitric and Eutric Andosols developed in similar basaltic ash, but with contrasting mineral and physico-chemical properties. These soils constitute a weathering sequence, from the young, undifferentiated Vitric Andosols to the well-developed Eutric Andosols.

Pyroclast weathering has led to Si depletion, relative accumulation of Al and Fe, formation of secondary minerals, and hence the development of large specific surfaces in the Eutric Andosols.

Continuous acid inputs have decreased the pH of both the Vitric and Eutric soils, while favouring the development of positive charges at the surface of Al and Fe oxyhydroxide and allophane minerals. In turn, this has permitted loss of alkaline and alkaline-earth cations through displacement from exchange sites. However, the continuous inputs of volcanogenic acid have had a negligible effect on ANC_s, but affected soil physico-chemical properties. Similarly, despite large concentrations of sulphur in the soils, total SO_3 content affected ANC_s little in young Vitric Andosols, but caused an increased contribution to ANC_s in Eutric Andosols. In addition, inorganic sulphate retention may retard net acidification of the soil. A correct assessment of the inorganic pool of S in these highly S-retentive Andosols is therefore of fundamental importance.

Despite the larger ANC_s of the Vitric compared to the Eutric Andosols, soil pH was less in the Vitric than in the Eutric Andosols because the mechanisms involved in the regulation of volcanic acid flux are different: mineral weathering is the dominant process in Vitric Andosols, whereas cation exchange and sulphate sorption would significantly contribute to regulating proton consumption in Eutric Andosols.